

Structural Design, Analysis and Optimisation of Robotic Arm

Er. Sandeep Chowdhry¹

¹Engineering Consultant & Trainer, Chandigarh, India

Abstract – The structural elasticity and the vibrations in the links are two leading causes that significantly affect the performance of the Robotic Arm. This study aims to design a structurally stable Robotic arm with higher natural frequencies and low mass. Finite Element Analysis (FEA) is used to find the modal frequencies. Response Surface Method (RSM) is used to optimise the process variables. The result findings show that link 1 thickness has a more significant effect on the natural frequencies and the mass of the Robotic Arm than the thickness of link 2. Second, to increase the structural strength of the Robotic Arm, link 2 may be designed lighter in weight than link 1.

Key Words: Robotic Arm, RSM, FEA, Structural Design, Modal Analysis

1. INTRODUCTION

In this study, a Robotic Arm is designed for tracking and force control for education purposes. The design objectives for the complete arm include three degrees of freedom, a large (0.98 m to 1.8 m) workspace, 4 kg payload capacity, electrical actuation and mechanical simplicity. Specific design objectives arising from the proposed application include the following 1) Precise joint level torque control; 2) High structural vibration frequencies; 3) High stiffness; 4) Low weight; 5) High static strength. The inclusion of the robot structural strength constraint in the optimisation helps in reducing mass effectively. It also addresses the fatigue limit, a significant concern in robot systems, by conducting fatigue simulation in FEA module [1]. The robotic arm's structural elasticity and the torque ripple of permanent magnet motors degrade the fidelity of joint level torque control and cause oscillations in the position and force control loops [2]-[6]. [6] suggested that careful motor design and structural design optimisation [7][8] can lead to arm design exhibiting superior force and position tracking performance. When the operating frequency of the system is near the natural frequency is one of the reasons for the system's vibration [9]. Therefore, designing the robotic arm with a high natural frequency is essential. Arm design possessing high structural vibration frequencies while carrying a gripper payload also satisfies the objectives of low mass, high stiffness and high strength [10]. However, it is not clear whether high structural vibration frequencies will automatically optimise the mass of both links. As a result, in this study, high structural vibration frequencies and mass are selected as the response variables. This research aims 1) To present the mechanical design and supporting structural

FEA data for a new high-performance robot arm; 2) to Maximise the Robotic Arm's natural vibration frequencies; 3) to Minimise the mass of the Robotic Arm. This study aims to contribute to the literature on the Robotic Arm's design, analysis, and optimisation.

2. KINEMATIC MECHANISM

The band-drive mechanism is chosen for the Robotic Arm. This design provides excellent vibrational characteristics at all joint positions. Moreover, it can be optimised to exhibit fundamental modes that are nearly identical at all joint positions. Second, the design is mechanically simple and easy to fabricate. Third, an optimised band drive design will be significantly lighter than the alternative designs [10]. In this design, both motors are mounted directly on the base to reduce their gravitational and inertial coupling. Link1, the proximal link is directly operated by motor 1 and link 2, the distal link is actuated by motor 2 through 1:1 pre tensioned steel band and pulley arrangement.

3. MECHANICAL DESIGN

3.1 MOTOR DESIGN

The electric motor design task is simplified by selecting NEMA 23S stepper motors to drive both the links. It has 2500 rpm, holding torque at peak current of 1.3 Nm, step angle of 1.8° and weighs 0.80 kg.

3.2 LINK DESIGN

The length of the two links is selected as 0.49m. The cross-sections of both the links are chosen to be square tubular. The outer cross-sectional dimensions of link1 and link 2 are chosen to be 0.13m and 0.94m, respectively. The pulley diameter is 0.16m. The materials used for the links and the pulleys is aluminium-6061 and steel, respectively. Fig. 1 shows the Robotic Arm assembly without a gripper. The finite element method (FEM) based design optimisation procedure described in the next section dictates the local wall thickness of both links.

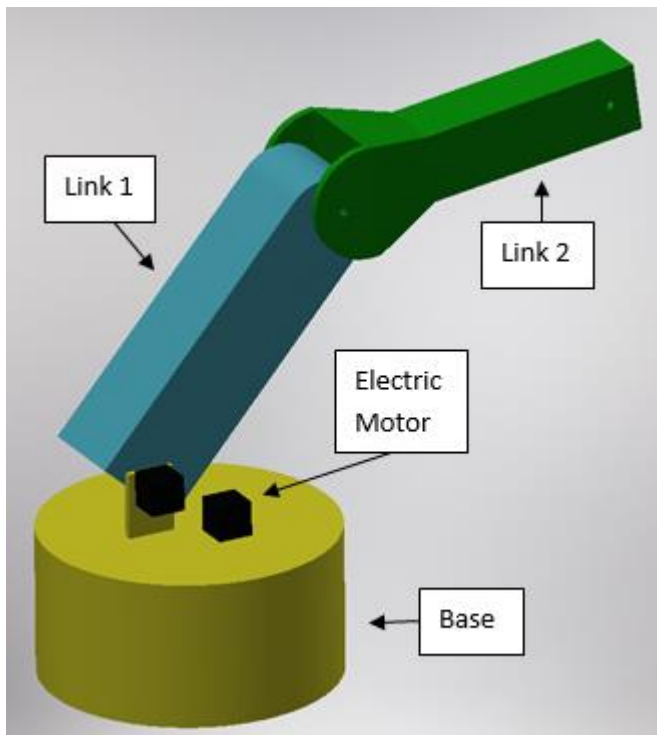


Fig -1: Robotic Arm without a gripper

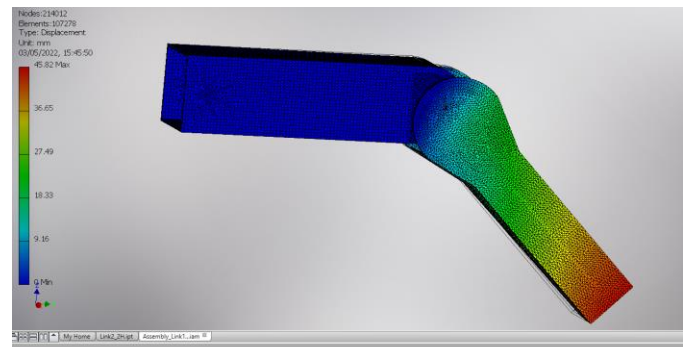


Fig -3: Robotic Arm model with link 1 and link 2 joint angle at 45°

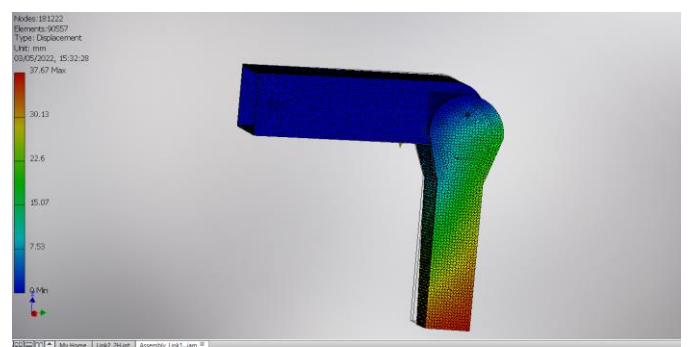


Fig -4: Robotic Arm model with link 1 and link 2 joint angle at 90°

3.3 FINITE ELEMENT MODEL (FEM)

Autodesk Inventor Professional 2016 software’s design, simulation and solution modules are used for the FEM analysis. The first mode of the fundamental frequencies of the Robotic Arm free to rotate will be approximately three times higher than the cantilever case (locked). Therefore, the conservative approach to modelling joints is locked for the FEA simulation. Both the motors are modelled as rigidly connected (cantilever) to the base. The base is modelled as cantilevered to the ground. To simplify, the fixed base of the Robotic Arm is not used in the FEA. A fixed constraint is applied at the end of link1. The spring elements representing the pre-tensioned steel band are also cantilevered. The validity and appropriateness of these boundary conditions of this model are addressed in [11][12]. Fig. 2, Fig.3 and Fig. 4 shows the FEA results of the Robotic Arm model with link 1 and link 2 joint angles at 0°, 45° and 90°, respectively.

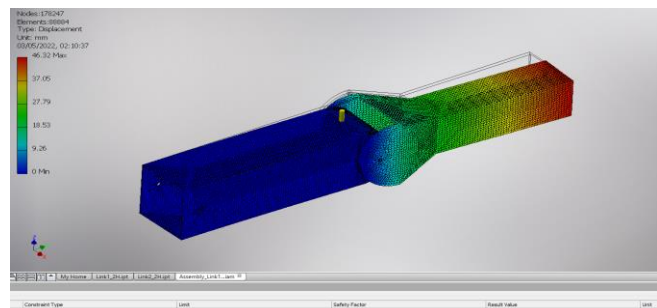


Fig -2: Robotic Arm model with link 1 and link 2 joint angle at 0°

4. OPTIMISATION

4.1 Optimisation invariants

The following parameters are invariant, 1) link 1 and link 2 each of length 0.49m; 2) link 1 and link 2 material is aluminium-6061; 3) link 1 and link 2 have square tubular cross-section; 4) link 1 and link 2 cross-sections are 0.13m and 0.094m respectively.

4.2 Optimisation variable

The thickness link 1 and link 2 are optimised to maximise the first natural frequency and minimise the mass of the Robotic arm for the overall structure with a 4kg gripper payload. This approach is similar to [13] for the single-link manipulator. The Robotic Arm is analysed for the robot gripper carrying no load and the robot gripper carrying a 4kg payload. Although fundamental frequencies are independent of joint 1 (between the base and link 1), the entire range of the joint 2 (between link 1 and link 2) positions are explored as shown in Fig. 2, Fig. 3 and Fig.4.

4.3 Parameters, Levels and Responses

Table 1 shows the level settings of the thicknesses of link 1 and link 2 of the robotic arm. The first natural frequency (Hz) and the mass (kg) of the robotic arm is selected as the response.

Table -1: Process parameter levels

Process Parameter	Low Level	High Level
Link 1 (mm)	4	16
Link 2 (mm)	4	11

4.4 Response Surface Method (RSM)

Minitab 2019 software is used to design the run order for the Response Surface Method (RSM). The Central Composite Design (CCD) consists of 8 factorial points and six centre points or 14 points (Run 1-14) with one replicate and two blocks. The CCD is shown in Table 2.

Table -2: Central composite design of RSM

Run Order	Link 1 (mm)	Link 2 (mm)
1	18.49	7.5
2	10	7.5
3	10	7.5
4	1.51	7.5
5	10	7.5
6	10	12.45
7	10	2.55
8	10	7.5
9	4	4
10	10	7.5
11	16	4
12	16	11
13	10	7.5
14	4	11

4.5 Procedure

The Robotic Arm assembly is transferred to the Stress Analysis environment in Autodesk Inventor Professional 2016 to perform modal analysis. Aluminium-6061 is selected as the material for the Robotic Arm. A fixed constraint is applied at the end of link 1. Gravity load is applied to the Robotic arm. Mesh element size is 0.025 to get accurate results. In the first run, the thicknesses of link1 and 2 are

selected as per Table 2. The simulation result of first vibration frequency and the mass of the Robotic Arm is recorded. Similarly, the response values are recorded for all the run orders. Afterwards, Minitab software is used to analyse the response surface design with a confidence level of 95% ($\alpha=0.05$). The residual plots showed that the errors are random, independent, normally distributed and have constant variance across all factor levels.

5. RESULTS

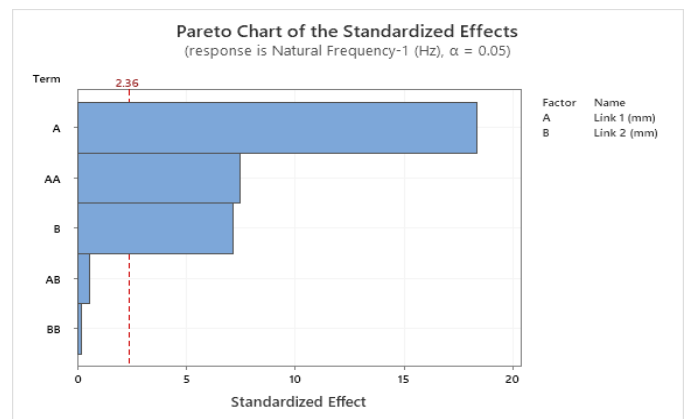


Fig -5: Significant parameters for natural frequency

The Pareto chart (Fig. 5) shows that the thickness of link 1, the thickness of link 2 and the square of the thickness of the link1 are significant at $\alpha = 0.05$. The square of link 2 thickness and the interaction between the thickness of link 1 and the thickness of link 2 are insignificant at $\alpha = 0.05$. The refined regression equation with $R^2 = 98.45\%$ is,

$$\begin{aligned} \text{Natural Frequency-1 (Hz)} &= 107.11 + 15.58 \text{ Link 1 (mm)} - \\ & 4.307 \text{ Link 2 (mm)} \\ & - 0.4559 \text{ Link 1 (mm)*Link 1 (mm)} \end{aligned}$$

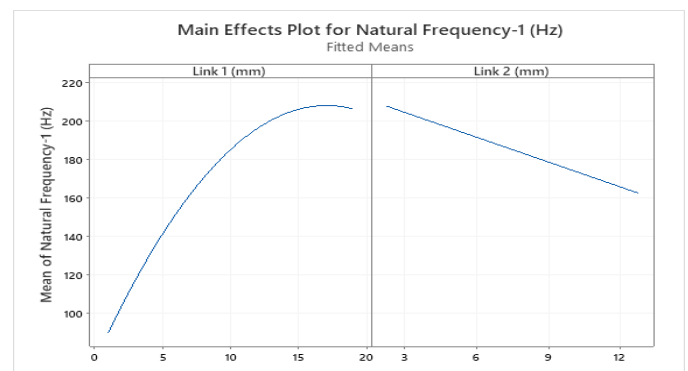


Fig -6: Main effect of thicknesses of link 1 and link 2 on Natural Frequency

The main effect plots (Fig. 6) show that the link 1 thickness has a non-linear relationship with the first natural frequency. Second, link 2 thickness has a linear relationship with the first natural frequency.

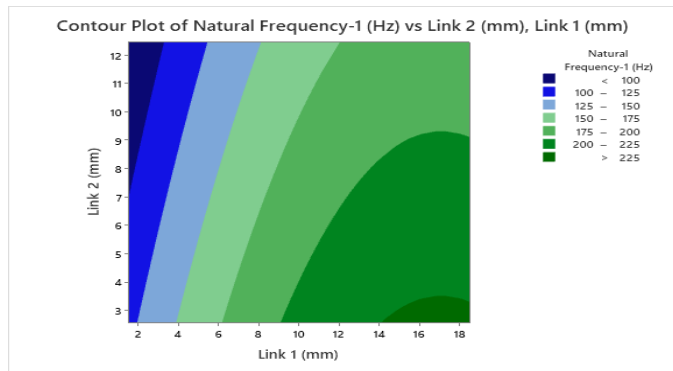


Fig -7: Surface plot of both links thickness with Natural Frequency

The surface plots (Fig. 7) show a decrease in the link 2 thickness, and increased link 1 thickness leads to the higher natural frequency.

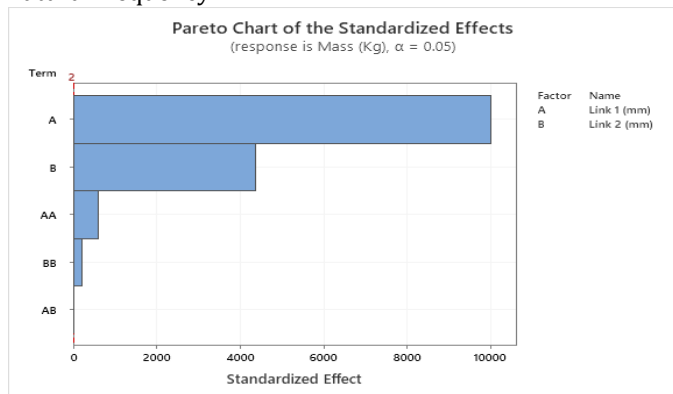


Fig -8: Significant parameters for mass

The Pareto chart (Fig. 8) shows that thickness of link 1, thickness of link 2, square of thickness of link 1 and square of thickness of link 2 significantly affect the mass at $\alpha = 0.05$. The interaction between thickness of link 1 and thickness of link 2 has insignificant affect on the mass at $\alpha = 0.05$.

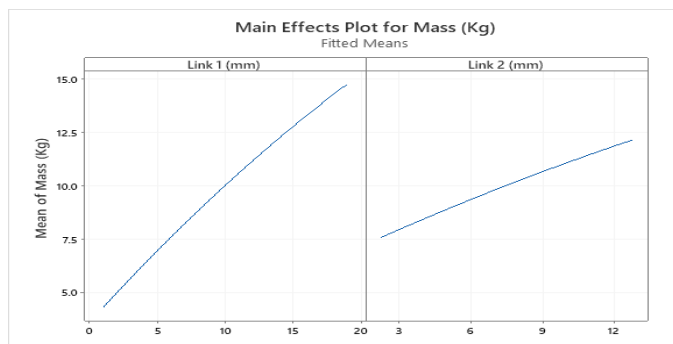


Fig -9: Main effect of thicknesses of link 1 and link 2 on mass

The main effect plots (Fig. 9) show that the link 1 and link 2 thickness have a non-linear relationship with the first natural frequency.

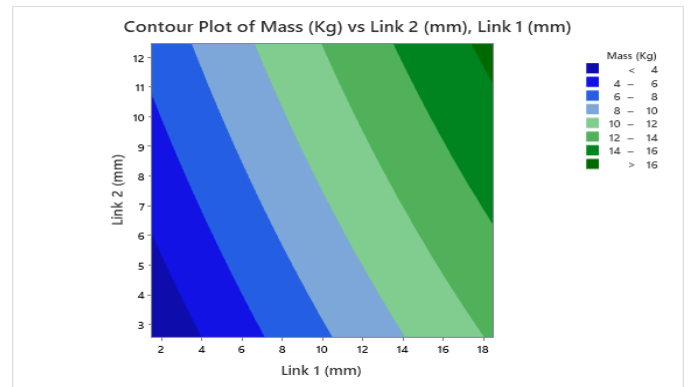


Fig -10: : Surface plot of both links thickness with mass

The surface plots (Fig. 10) show a increase in the link 1 thickness, and an increased link 2 thickness leads to an increase in the mass.

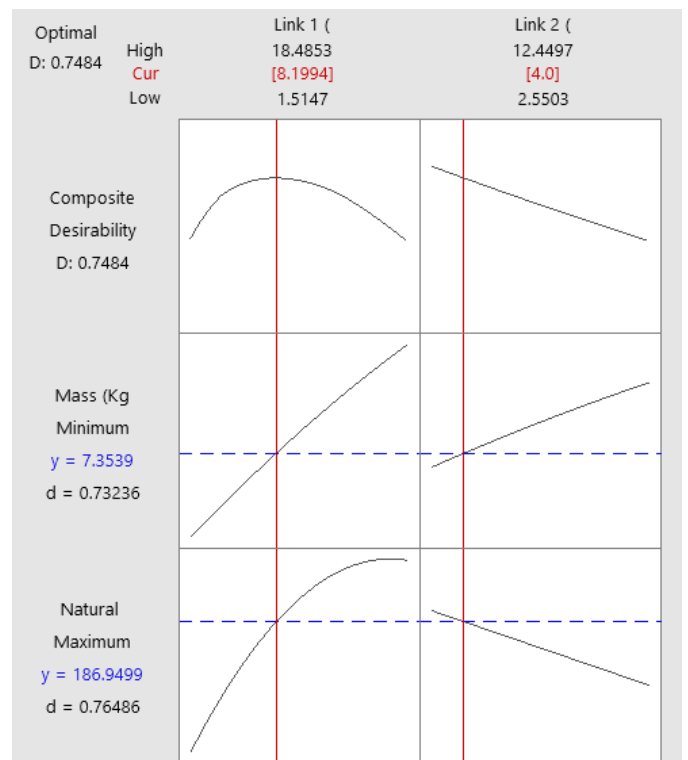


Fig -11: Optimised thicknesses of both the links

The optimisation graph (Fig. 11) shows that with link 1 thickness of 8.1994 mm and link 2 thickness of 4 mm, the maximum natural frequency value obtained is 186.9499 Hz. The minimum mass is 7.3539 kg.

6. DISCUSSION

The thickness of link 1 has a non-linear relationship with the natural frequency (Fig. 6) and the mass (Fig. 9). In addition, the slope of the curves is steeper than the curves of the thickness of link 2. It shows that link 1 thickness has a more considerable effect on the natural frequency and mass of the robotic arm than the thickness of link 2. Therefore, to improve the performance of the Robotic Arm care may be taken to design the link 1. Second, the optimisation graph (Fig. 11) shows that higher natural frequency does not lead to low mass. As a result, this finding is in disagreement with [10]. Third, the gripper payload is applied as a point load. The results show that the payload did not affect the natural frequencies. Fourth, the different orientations of the joint angle between link 1 and link 2 did not affect the natural frequencies. This finding is in agreement with [10]. Fifth, the inverse relationship between the link 2 thickness and the natural frequency indicates that link 2 may be designed lighter in weight than link 1 to increase the structural strength of the Robotic Arm.

7. CONCLUSIONS

This research reported the mechanical design of the Robotic Arm links. The study also provided supporting modal analysis data for the Robotic Arm. Detailed findings presented in section 5 and section 6 are summarised here.

1) Link 1 may be designed carefully to improve the performance of the Robotic Arm because the thickness of link 1 has a more considerable effect on the natural frequency and the mass of the Robotic Arm. 2) Higher natural frequency does not automatically select the low mass for the links. 3) To increase the structural stability of the Robotic Arm, link 2 may be designed to be lighter in weight compared to link 1. 4) Joint orientation of link 1 and link 2 did not affect the natural frequencies. Limitation of this study is that kinematics and dynamics is not considered in the optimisation. A suggested direction for future research is to perform the structural design optimisation of the Robotic Arm under the dynamic loads.

REFERENCES

- [1] Design optimisation of a light-weight robotic arm under structural constraints Shaoping Bai and Lelai Zhou Department of Mechanical and Manufacturing Engineering Aalborg University, Aalborg, Denmark e-mail: {shb,lzh}@m-tech.aau.dk
- [2] N. M. Kircanski and A. A. Goldenberg, "An experimental study of nonlinear stiffness, hysteresis, and friction effects in robot joints with harmonic drives and torque sensors," *Int. J. Robot. Res.*, vol. 16, no. 2, pp. 214–239, 1997.
- [3] H. Schemph, "Comparative design, modelling, and control of robotic transmissions," Ph.D. dissertation, Dept. Appl. Ocean Phys. Eng., Woods Hole Oceanographic Institution,

Woods Hole, MA, and Massachusetts Institute of Technology, Cambridge, 1990.

- [4] L. L. Whitcomb, A. Rizzi, and D. E. Koditschek, "Comparative experiments with a new adaptive controller for robot arms," *IEEE Trans. Robot. Automat.*, vol. 9, pp. 59–70, Feb. 1993.
- [5] G. Ferretti, G. Magnani, and P. Rocco, "Force oscillations in contact motion of industrial robots: An experimental investigation," *IEEE/ASME Trans. Mechatron.*, vol. 4, pp. 86–91, Mar. 1999.
- [6] D. Hanselman, J. Hung, and J. M. Keshura, "Torque ripple analysis in brushless permanent magnet motor drives," in *Proc. Int. Conf. Electric Machines*, Manchester, U.K., Sept. 1992, pp. 823–827.
- [7] H. Asada and K. Youcef-Toumi, *Direct-Drive Robots: Theory and Practice*. Cambridge, MA: MIT Press, 1987.
- [8] H. Sekiguchi and K. Takeshita, "Vibration analysis of SCARA type direct-drive robot with double link mechanism," *J. Japan Soc. Prec. Eng.*, vol. 55, no. 2, pp. 387–392, 1989.
- [9] R. Pan, C. Hu, J. Fan, Z. Wang, X. Huang and F. Lu, "Study on optimisation of the dynamic performance of the robot bonnet polishing system," Beijing, 2022.
- [10] Jaydeep Roy and Louis L. Whitcomb, Comparative Structural Analysis of 2-DOF Semi-Direct-Drive Linkages for Robot Arms, IEEE/ASME TRANSACTIONS ON MECHATRONICS, VOL. 4, NO. 1, MARCH 1999 PP 82-86.
- [11] J. Roy and L. L. Whitcomb, "Comparative structural analysis of 2-DOF semi-direct-drive linkages for robot arms," *IEEE/ASME Trans. Mechatron.*, vol. 4, pp. 82–86, Mar. 1999.
- [12] J. Roy and L. L. Whitcomb, "Structural design optimisation and comparative analysis of a new high-performance robot arm via finite element analysis," Johns Hopkins University, Department of Mechanical Engineering, Dynamics and Control Laboratory, Baltimore, MD, Tech. Rep. 9801, 1998.
- [13] A. Pil and H. Asada, "Rapid recursive structure redesign for improved dynamics of a single link robot," *ASME J. Dynam. Syst., Measure., Contr.*, vol. 117, no. 4, pp. 520–526, Dec. 1995.

BIOGRAPHIES



Er. Sandeep Chowdhry has done Bachelor of Engineering in Mechanical Engineering with a Specialisation in Manufacturing Engineering from S.L.I.E.T. Punjab, India and is interested in solving industrial problems and imparting training to the professionals in the industry.